The effects of waves on the jets of a Sewage outfall diffuser

Mossa A., Petrillo A.F.

in

Camarda D. (ed.), Grassini L. (ed.).
Coastal zone management in the Mediterranean region

Bari : CIHEAM
Options Méditerranéennes : Série A. Séminaires Méditerranéens; n. 53

2002
pages 77-87

THE EFFECTS OF WAVES ON THE JETS OF A SEWAGE OUTFALL DIFFUSER

M. Mossa, A.F. Petrillo
Dipartimento di Ingegneria Civile e Ambientale, Politecnico di Bari, Italy

ABSTRACT

This paper presents experimental results of a turbulent neutrally-buoyant jet vertically discharged in a stagnant ambient and of the same jet discharged in a flow field of regular waves. The study was carried out in the wave channel at the laboratory of the Department of Civil and Environmental Engineering (Water Engineering Division) of Bari Polytechnic. Initial conclusions are reported in Mossa (1996). Velocity jet components were measured with a backscatter, two-component four-beam LDA system. The main results of the present study indicate the following: 1) Comparison of the root-mean square of turbulent velocity components indicates the effect of wave presence. Particularly, the root-mean square of turbulent velocity components for sections further from the nozzle are consistently greater than those of the same jet discharged in stagnant ambient. 2) The root-mean square of the turbulent velocity components of jets in wave environment are greater than for the same jet in stagnant ambient, at least in cross sections particularly far from the nozzle. 3) For cross sections further from the nozzle, the experimental values of shear turbulent Reynolds stresses indicate that for configurations with the presence of wave motions, an inversion of the sign compared to the jet issued in quiescent ambient occurs.

1. INTRODUCTION

The sea has for always been the ultimate sink for water-borne waste products coming from the land. In recent years the effects on the processes of mixing and transportation, such as jet momentum, buoyancy, current, stratification, etc., had received more and more attentions from the scientists; but the wave action also play a very important role in many cases (Shuto and Ti, 1974; Ger, 1979; Sharp, 1986). While there are several studies in literature on non-buoyant and buoyant jets and their interaction with currents (Rajaratnam, 1976), few deal with jet-wave interaction, with the majority emphasizing the importance of a wave flow field in diffusion processes (Chin, 1987; Chyan and Hwung, 1993; Koole and Swan, 1994a; Koole and Swan, 1994b; Hwung et al., 1994; Mossa, 1996; Mossa and Petrillo, 1997; Wu et al., 1998) and the necessity of experimental tests to explain jet-wave interaction dynamics and possibly confirm the validity of mathematical models present in literature (Chin, 1988).

The present paper is to be considered in the context of Mossa's research (1996) and represents the direct continuation of the initial results reported in that work.

2. EXPERIMENTAL SET-UP

Experiments were carried out in a wave channel at the laboratory of the Civil and Environmental Engineering Department (Water Engineering Division) of Bari Polytechnic (Italy). The channel is about 45 m long and 1 m wide; its wall is made up of crystal plane sheets 1.2 m high, supported by iron frames with a center-to-center distance of about 0.44 m, where resistance probes for wave profile measurements may be placed. During testing, mean water depth near the paddle was h=0.8 m. The velocity field was measured by using a backscatter, two-component four-beam fiber-optic LDA system. A 5 W water-cooled argon-ion laser, a transmitter, a 85 mm probe (focal length 310 mm, beam spacing 60 mm) and Dantec 58N40 FVA Enhanced signal processor were used. The accuracy of velocity measurements is ±2%. For jet-wave interaction configurations, the measurement system allows us to assess, at the same time as the velocity components, the wave elevation profile, by use of a resistance probe placed in a transversal section of the channel crossing the laser measurement volume. The entire system is assisted by a process computer.

This study was carried out for a jet discharged in a stagnant ambient and for the same jet interacting with progressive wave flow fields.

The vertical non-buoyant jet was introduced through a 2.01 mm in-diameter nozzle, with volume flow rate equal to 22.22 cm^3/s, discharge velocity U_o equal to 6.42 m/s and Reynolds number equal to 13482. The round nozzle was located at about 11 m from the wavemaker at 16.7 cm from the bottom of the channel. As for wave motion, regular wave trains were reproduced in the channel characterized by periods for each configuration of 2.00 s, 1.43 s and 1.00 s respectively. Table 1 reports wave height (*H*), wave length (*L*), period (*T*), *H/L* and *h/L* parameters, relative to configurations with wave motion for which velocity surveys were made. The wave flow field in the channel can be described with Stokes II order theory according to the classic Le Méhauté abacus (1969). The reflection coefficient in the channel is not greater than 9%. For each configuration we measured the vertical and horizontal velocity components at points of the longitudinal section of the channel that crosses the nozzle. The cross sections of the jet, along which measurements were carried out, were 5, 10, 60, 110, 160, 210, and 260 mm from the nozzle, with the exception of configurations 2 and 3 in Table 1, for which measurements were carried out in sections 5, 60, and 110 mm from the nozzle. For some jet cross sections, velocity measurements were carried out on both sides in order to verify symmetry and/or antisymmetry conditions of the flow field with respect to the jet axis. For a more detailed description of the experimental set-up see Mossa (1996).

Table 1. Main characteristics of the wave motion fields

Case	H [cm]	L [m]	T [s]	H/L	h/L
1	4.20	5.10	2.00	0.0082	0.1569
2	4.40	3.05	1.43	0.014	0.2623
3	4.13	1.56	1.00	0.027	0.5128

3. THEORETICAL BACKGROUND

The fundamental equations governing the problem can be derived from the Navier-Stokes equation. Any physical quantity is split into the steady mean flow component, the fluctuation component due to the statistical contribution of the wave and the fluctuation component of the turbulence (see, for example, Hussain and Reynolds, 1970). Therefore, the u_i component of velocity can be expressed as follows:

$$u_i(x_i,t)=\langle u_i\rangle(x_i,t)+u_i'(x_i,t)=U_i(x_i)+\tilde{u}_i(x_i,t)+u_i'(x_i,t) \tag{1}$$

where the angular brackets < > are an operator to take an ensemble average, the tilde symbol indicates fluctuations due to the wave statistical contribution (or oscillating components), the prime symbol indicates turbulent fluctuations and capital letters or the over-bar indicates the steady mean flow (time-averaged components). Moreover, *t* is the time quantity, and x_i (i=1,2,3; x_1=*X*, x_2=*Y*, x_3=*Z*) are the coordinates of a Cartesian frame with *Z* extending positive upwards from the orifice, *X* is the longitudinal axis extending positive onshore and *Y* is normal to the former two. The velocity components that were measured in the present study are $u_1=v$ in the *X* direction (cross velocity component, conventionally established as positive if oriented toward the shore) and $u_3=u$ in the *Z* direction (longitudinal velocity component, conventionally established as positive if oriented upward).

In the present study for the cases of jets interacting with waves ensemble-averaged velocities were obtained by phase-averaging the measured signals separated by the wave period over about five hundreds waves. The results, which represented the phase-averaged velocities at different phases of a wave cycle, were averaged to yield the time-averaged velocities. Turbulent velocity fluctuations were obtained by subtracting phase-averaged velocities from the original time series

In this section the equations of motion for turbulent non-buoyant jet flow under wave action will be developed. Using the Cartesian tensor notation, the classic equations of motion of an incompressible fluid are

$$\frac{\partial u_i}{\partial t}+\frac{\partial u_j u_i}{\partial x_j}=\frac{1}{\rho}\frac{\partial}{\partial x_j}\sigma_{ij} \tag{2}$$

$$\frac{\partial u_i}{\partial x_i} = 0 \tag{3}$$

The stress tensor σ_{ij} is defined as follows

$$\sigma_{ij} = -p\delta_{ij} + 2\mu s_{ij} \tag{4}$$

where δ_{ij} is the Kronecker delta, p is the hydrodynamic pressure and μ is the dynamic viscosity. The rate of strain is defined

$$s_{ij} = \frac{1}{2}\left(\frac{\partial u_i}{\partial x_j} + \frac{\partial u_j}{\partial x_i}\right) \tag{5}$$

Writing the velocities as reported in eq. (1) and getting ensemble averaging of eq. (2) we obtain

$$\frac{\partial \langle u_i \rangle}{\partial t} + \frac{\partial \langle u_i \rangle \langle u_j \rangle}{\partial x_j} = \frac{1}{\rho}\frac{\partial}{\partial x_j}\left(\Sigma_{ij} - \rho\langle u'_i u'_j \rangle\right) \tag{6}$$

where

$$\Sigma_{ij} - \rho\langle u'_i u'_j \rangle = -\langle p \rangle \delta_{ij} + 2\mu S_{ij} - \rho\langle u'_i u'_j \rangle \tag{7}$$

and

$$S_{ij} = \frac{1}{2}\left(\frac{\partial \langle u_i \rangle}{\partial x_j} + \frac{\partial \langle u_j \rangle}{\partial x_i}\right) \tag{8}$$

The motion is periodic, so the average over the period *T* of eq. (6) becomes

$$\frac{\partial \overline{\langle u_i \rangle \langle u_j \rangle}}{\partial x_j} = \frac{1}{\rho}\frac{\partial}{\partial x_j}\left(\overline{\Sigma_{ij}} - \rho\overline{\langle u'_i u'_j \rangle}\right) \tag{9}$$

Some useful properties between two signals *f(t)* and *g(t)* that follow from the basic definition are

$$\langle f' \rangle = 0,\ \overline{\tilde{f}} = 0,\ \overline{f'} = 0,\ \overline{\langle f \rangle} = \langle \overline{f} \rangle = \overline{f},\ \langle \tilde{f} g \rangle = \tilde{f}\langle g \rangle,\ \langle \overline{f} g \rangle = \overline{f}\langle g \rangle,\ \overline{\langle \tilde{f} g' \rangle} = \overline{\tilde{f} g'} = 0 \tag{10}$$

where the last one states that, on average, the background turbulence and the organized motion are uncorrelated.

Using the eqs. (1) and (10) and the continuity equation

$$\frac{\partial U_i}{\partial x_i} = 0 \tag{11}$$

we obtain

$$\frac{\partial}{\partial x_j}\left(U_i U_j + \overline{\tilde{u}_i \tilde{u}_j} + \overline{u'_i u'_j}\right) = \frac{1}{\rho}\left(\frac{\partial P}{\partial x_j}\delta_{ij} + \mu\frac{\partial^2 U_i}{\partial x_j \partial x_j}\right) \tag{12}$$

4. EXPERIMENTAL RESULTS

Figures 1a÷n report diagrams of root-mean square of the cross and longitudinal turbulent velocity components, where *x* is the distance from the jet axis. From the analysis of figures relative to the section 5 mm from the nozzle we may observe the existence of the core in the case of the jet issued in stagnant ambient. Indeed, the diagram presents a local minimum on the center line. As for configurations of jet-wave interaction, we may note the effect of the wave flow field near the nozzle. In fact, it is observable that the profile of the root-mean square presents a local minimum on the jet axis which is less evident than in the case of jet discharged in quiescent ambient. Furthermore, we observed that the profile shows lower values as the wave period is reduced.

Figure 1c shows the absence in the jet with the presence of wave flow motion of the local minimum in the center line and lower value than those of the same jet discharged in quiescent ambient. In effect, for the jet cross section 10 mm from the nozzle and, generally speaking, for sections in the *deflection region* (Chyan and Hwung, 1993), the wave flow field causes the jet to oscillate even though it maintains many of its hydrodynamic characteristics, i.e. preserves its *identity*. The result of this type of interaction is a mixing of the characteristics typical of the jet in stagnant ambient and, therefore, of a flattening of these characteristics on the jet cross section. In sections 60 and 110 mm from the nozzle (*transition region*) we observed that the root-mean square of turbulent velocity components of jets in wave environment increases proceeding from the jet axis toward the external region. In general, we noted that the root-mean square of turbulent velocity components of jets issued in wave environment are smaller than those of the same jet discharged in stagnant ambient near the axis. On the contrary, they are greater in measurement points of the cross sections further from the jet axis. In addition, it is evident that the root-mean square of turbulent velocities of jet-wave interaction, especially for the longitudinal turbulent velocity components, tend to increase with the distance from the axis. The root-mean square increases as the wave period is reduced. Although still valid, these conclusions are not as evident for cross turbulent velocity components.

As for the cross sections of the *developed jet region* (Figs. 1i÷n), we observed that root-mean squares of both longitudinal and cross turbulent velocity components are greater than for the same jet discharged in a stagnant ambient.

Figures 2a÷f show cross-sectional profiles of crosscorrelations $\overline{u'v'}$, which represent the ratio between the time-averaged turbulent Reynolds shear stresses $\overline{\tau_{xz}}$ and the water density ρ. For sections 10 mm and 60 mm from the nozzle we observed that the absolute values of the shear turbulent Reynolds stresses are smaller for jets in wave environment than those of the same jet issued in stagnant water. Furthermore, it is possible to observe that $\overline{u'v'}$ decreases with the decrease

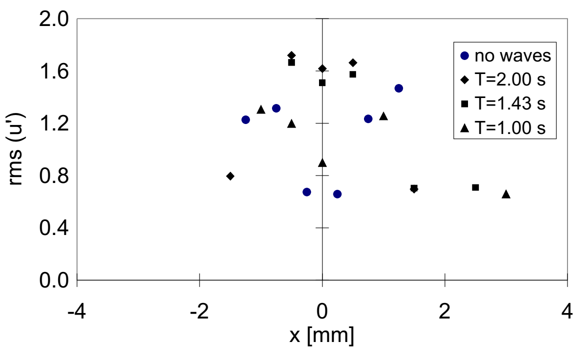

a) Cross section 5 mm from the nozzle.

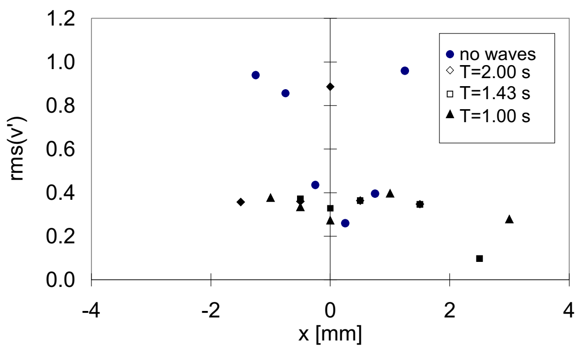

b) Cross section 5 mm from the nozzle.

Fig. 1. continued

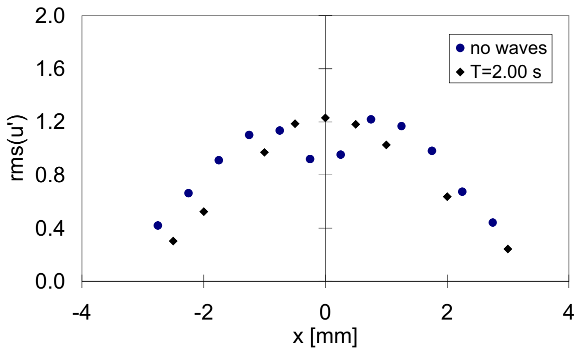

c) Cross section 10 mm from the nozzle.

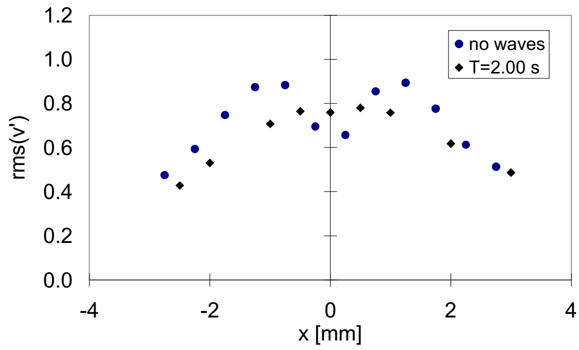

d) Cross section 10 mm from the nozzle.

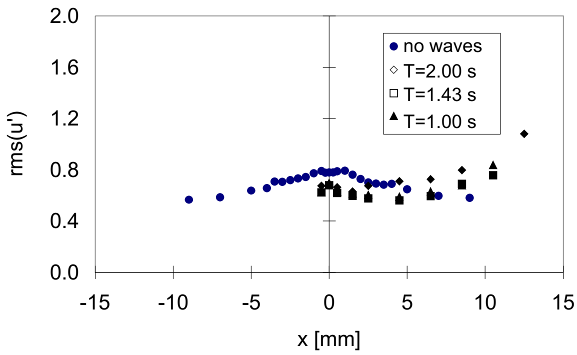

e) Cross section 60 mm from the nozzle.

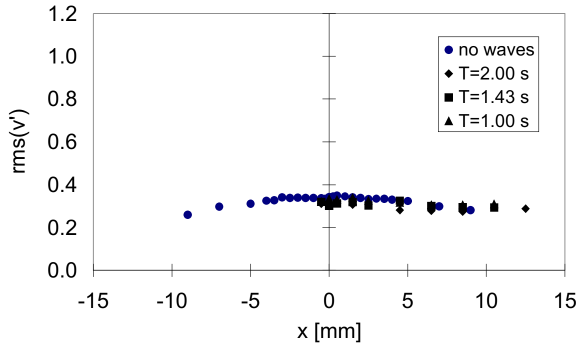

f) Cross section 60 mm from the nozzle.

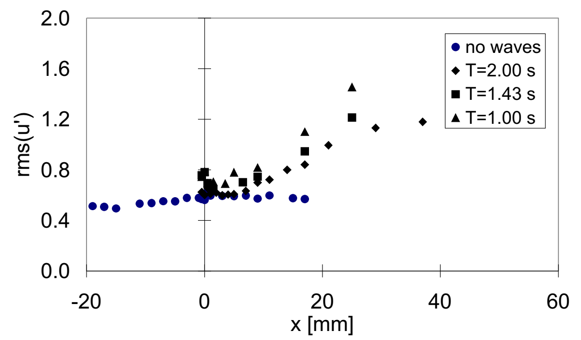

g) Cross section 110 mm from the nozzle.

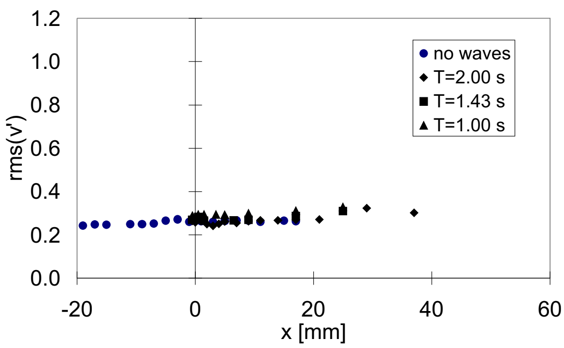

h) Cross section 110 mm from the nozzle.

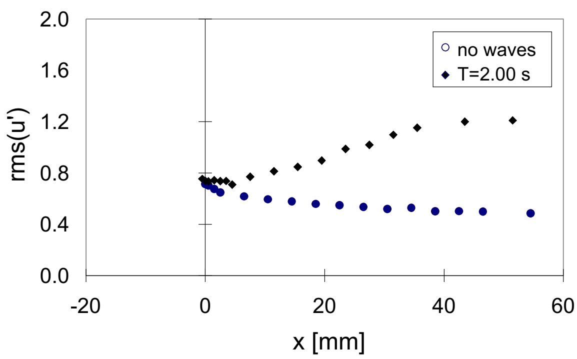

i) Cross section 160 mm from the nozzle.

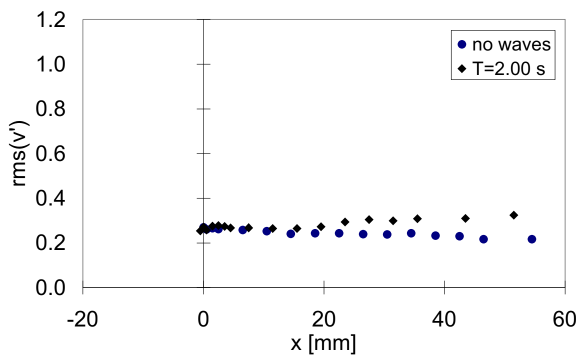

j) Cross section 160 mm from the nozzle.

Fig. 1. continued

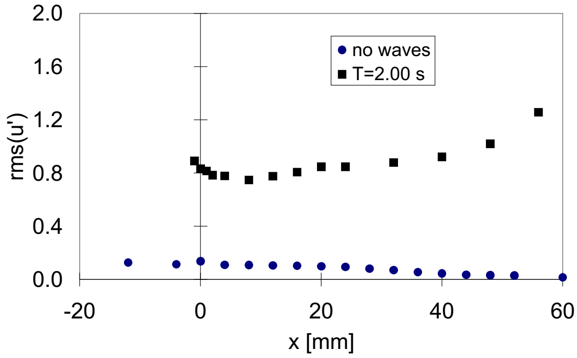

k) Cross section 210 mm from the nozzle.

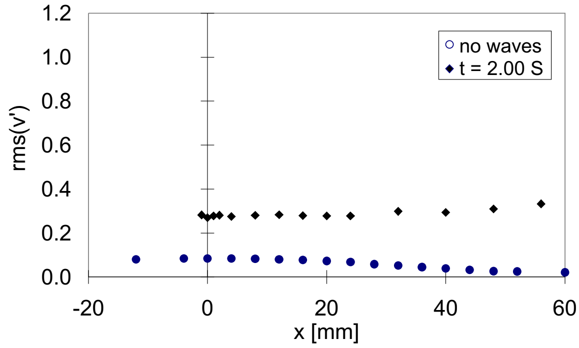

l) Cross section 210 mm from the nozzle.

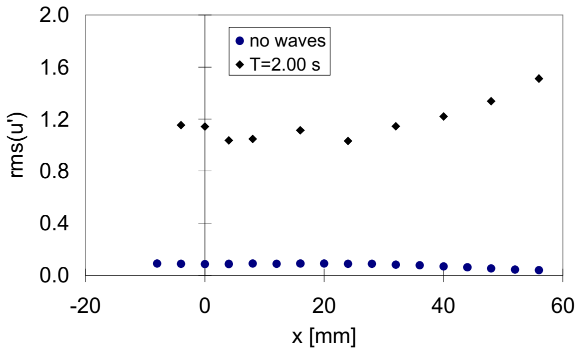

m) Cross section 260 mm from the nozzle.

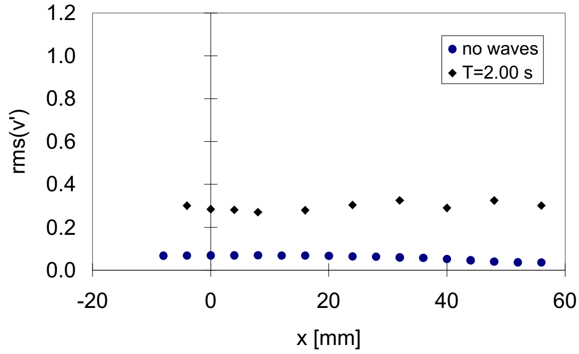

n) Cross section 260 mm from the nozzle.

Fig. 1. Cross-sectional profiles of root-mean square of turbulent vertical and horizontal velocity components.

of the wave period. In jet cross sections further away from the nozzle, $\overline{u'v'}$ values decrease even more, rendering it even more difficult to indicate clear trend in those sections, particularly for jet-wave interaction for which turbulent velocity values, in order to be educed, require numerical processing in higher numbers than jets discharged in still water. However, it is worth noting that jets in wave environment, starting from the cross section 210 mm from the nozzle, show an inversion of the sign of the time-averaged turbulent Reynolds shear stresses when compared to the same jet discharged in stagnant water. Indeed, starting from the jet cross section 210 mm from the nozzle, the profile of *U(x)* is flat near the axis (Mossa, 1996; Mossa, 1997), where therefore the contribution of $\partial U/\partial x$ in the equation of Boussinesq for the time-averaged shear turbulent Reynolds stresses becomes smaller than that of the same jet discharged in still water. Furthermore, in the sections in which the profile of *U(x)* presents twin peaks (see also Sharp, 1986 and Koole and Swan, 1994b), $\partial U/\partial x$ for measurement points near the axis has an opposite sign with respect to points further from the jet axis. At points in which the time-averaged shear turbulent Reynolds

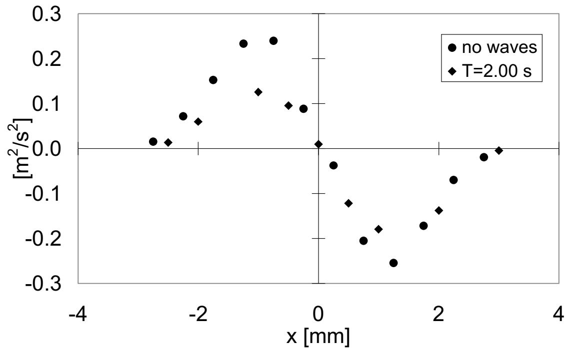

a) Cross section 10 mm from the nozzle.

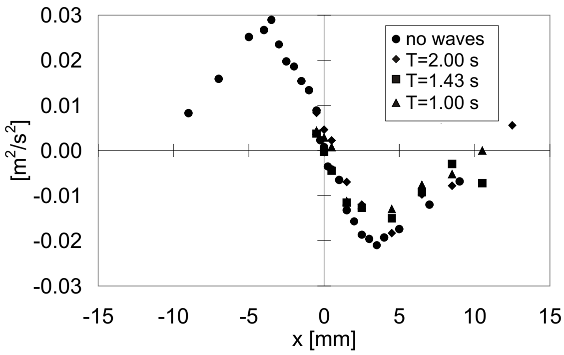

b) Cross section 60 mm from the nozzle.

Fig. 2. Continued

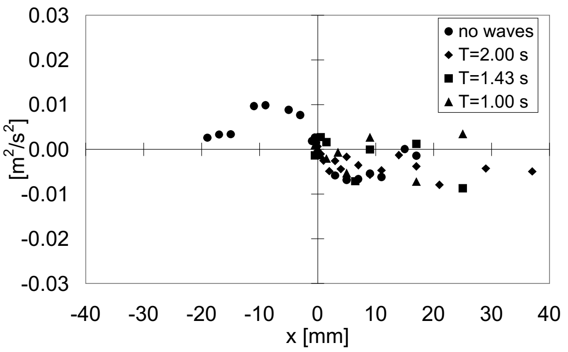

c) Cross section 110 mm from the nozzle.

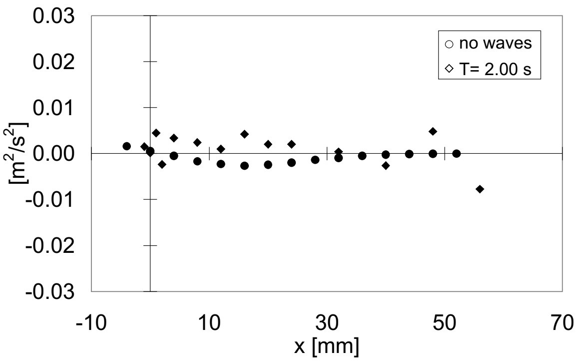

d) Cross section 160 mm from the nozzle.

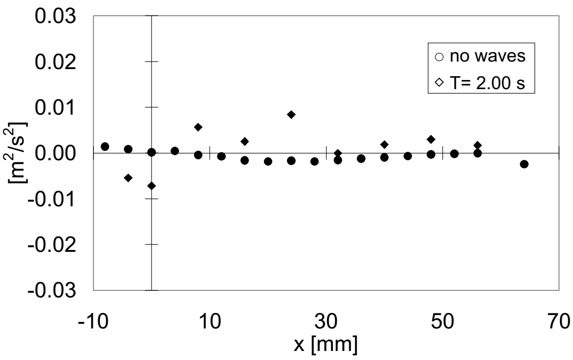

e) Cross section 210 mm from the nozzle.

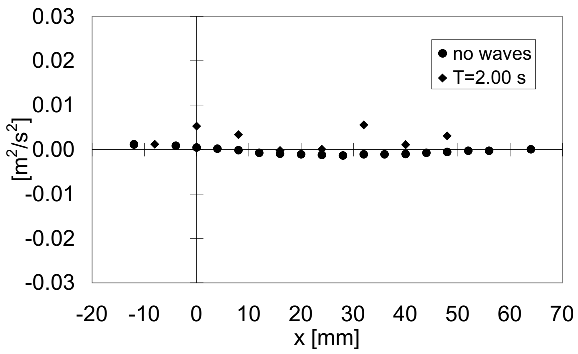

f) Cross section 260 mm from the nozzle.

Fig. 2. Cross-sectional profiles of $\overline{u'v'}$.

stresses of jet-wave interaction flow assume an opposite sign compared to those of the same jet discharged in a stagnant ambient, fluid flow further from the axis has an upwardly dragging effect on fluid near the axis, an observation confirmed by *U(x)* profiles, which show local minimum values in the jet center line.

Figures 3a÷n report cross-sectional profiles of $\overline{\tilde{u}^2}$ and $\overline{\tilde{v}^2}$ (i.e. ratio between normal Reynolds wave stresses and the water density). Both $\overline{\tilde{u}^2}$ and $\overline{\tilde{v}^2}$ present smaller values in the case of waves with smaller periods. We observed that $\overline{\tilde{u}^2}$ vanishes in the jet center line and presents a peak in intermediate positions between the jet axis and its external area.

Figures 4a÷f report cross sectional profiles of $\overline{\tilde{u}\tilde{v}}$ (i.e. ratio between shear wave Reynold stresses and the water density). Experimental analysis carried out showed that turbulent velocity components and those linked to (statistical) contribution of wave motion (oscillating velocity components) are not correlated, as foreseen by the latter in eqs. (10). Although the cross sectional

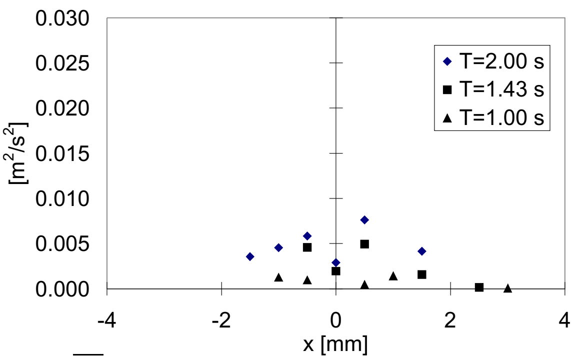

a) $\overline{\tilde{u}^2}$ at cross section 5 mm from the nozzle.

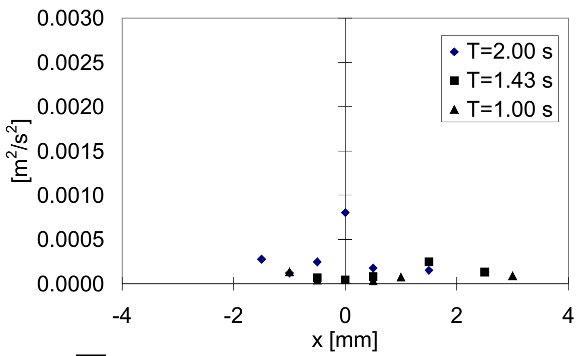

b) $\overline{\tilde{v}^2}$ at cross section 5 mm from the nozzle.

Fig. 3. Continued

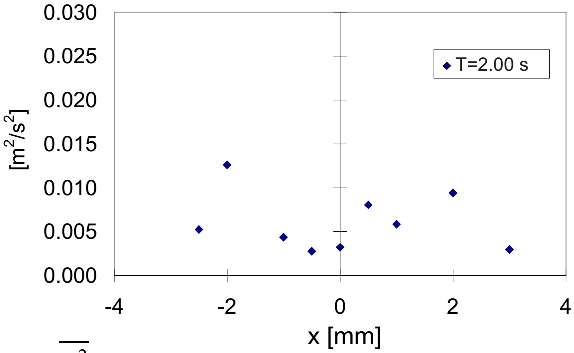

c) $\overline{\tilde{u}^2}$ at cross section 10 mm from the nozzle.

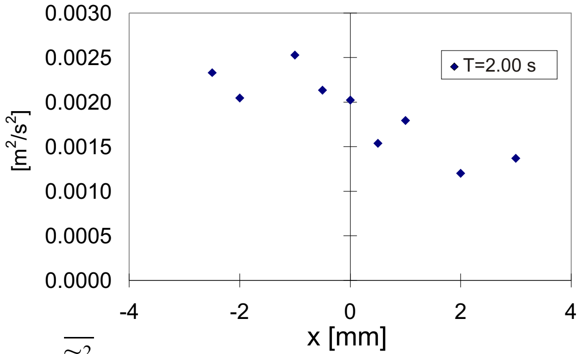

d) $\overline{\tilde{v}^2}$ at cross section 10 mm from the nozzle.

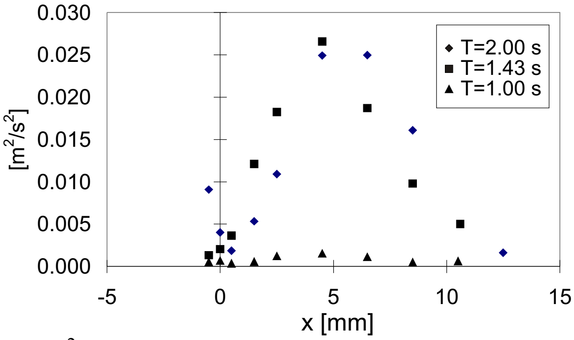

e) $\overline{\tilde{u}^2}$ at cross section 60 mm from the nozzle.

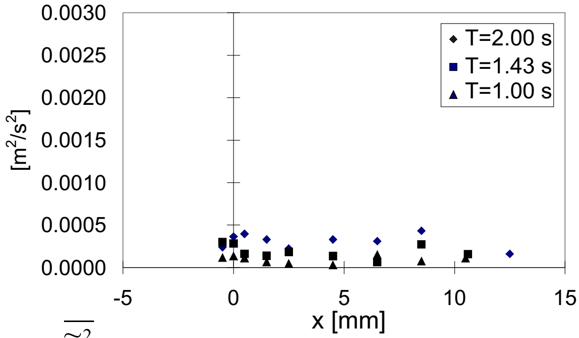

f) $\overline{\tilde{v}^2}$ at cross section 60 mm from the nozzle.

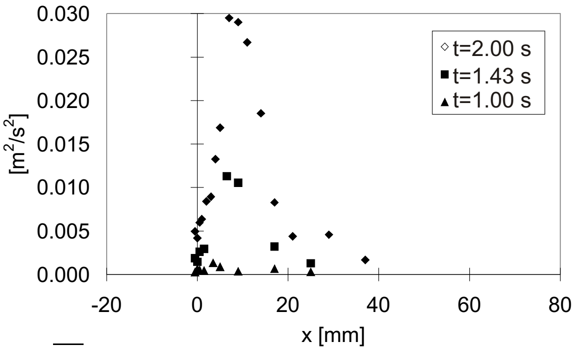

g) $\overline{\tilde{u}^2}$ at cross section 110 mm from the nozzle.

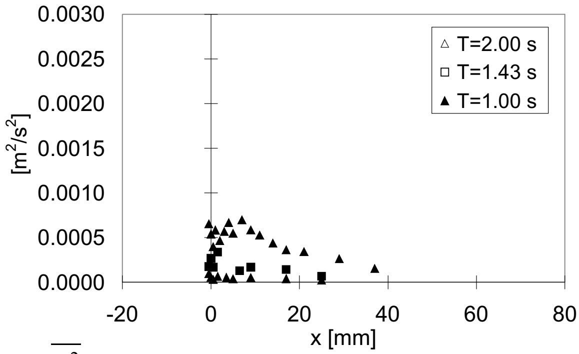

h) $\overline{\tilde{v}^2}$ at cross section 110 mm from the nozzle.

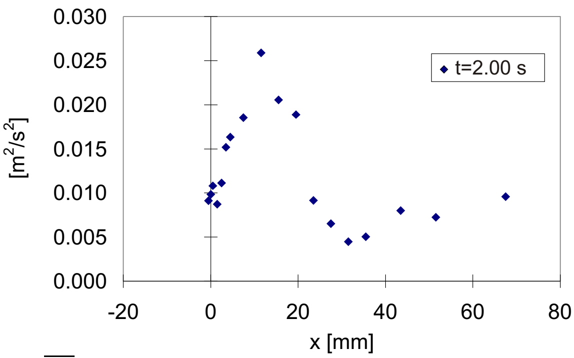

i) $\overline{\tilde{u}^2}$ at cross section 160 mm from the nozzle.

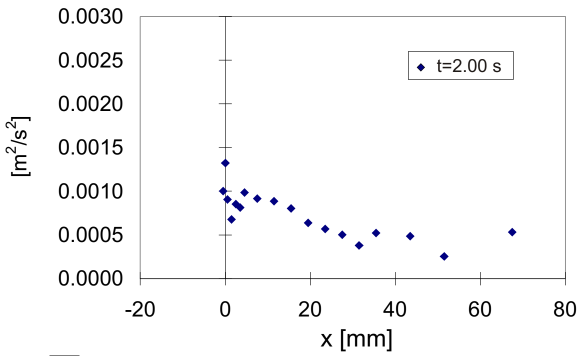

j) $\overline{\tilde{v}^2}$ at cross section 160 mm from the nozzle.

Fig. 3. Continued

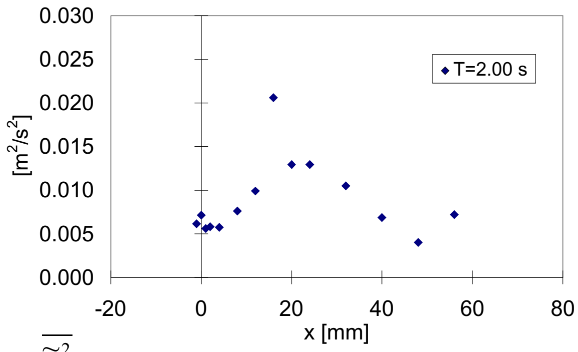

k) $\overline{\tilde{u}^2}$ at cross section 210 mm from the nozzle.

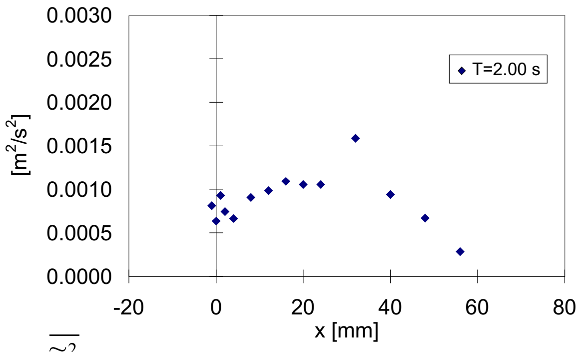

l) $\overline{\tilde{v}^2}$ at cross section 210 mm from the nozzle.

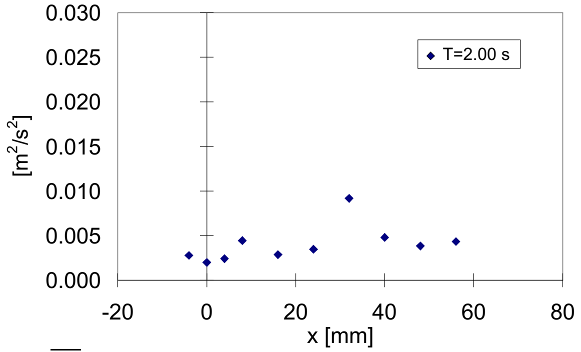

m) $\overline{\tilde{u}^2}$ at cross section 260 mm from the nozzle.

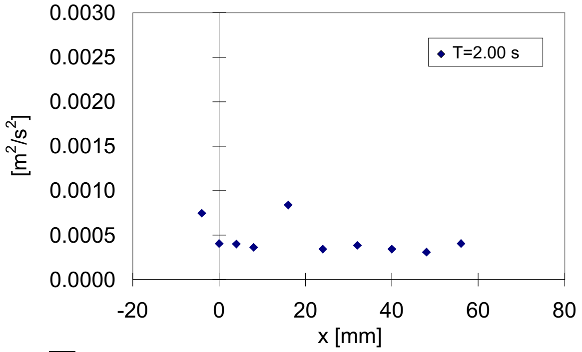

n) $\overline{\tilde{v}^2}$ at cross section 260 mm from the nozzle.

Fig. 3. Cross-sectional profiles of $\overline{\tilde{u}^2}$ and $\overline{\tilde{v}^2}$.

profiles of the shear wave Reynolds stress is similar to that of time-averaged shear turbulent Reynolds stresses, their magnitude is smaller. Comparison of the wave Reynolds stress in each cross section indicates that the lower the stress the smaller the wave period. From analysis of the previous figures we observed that the oscillating horizontal and vertical velocity components (linked to the statistical contribution of the wave motion field) are not always uncorrelated, as would be the case, on the contrary, in the hypothesis that they were described through Airy and Stokes II order theories.

5. CONCLUSIONS

The present study analyzes turbulent non-buoyant jets vertically discharged in a stagnant ambient and in the presence of wave motion. In particular, we have split the velocity acquired with LDA

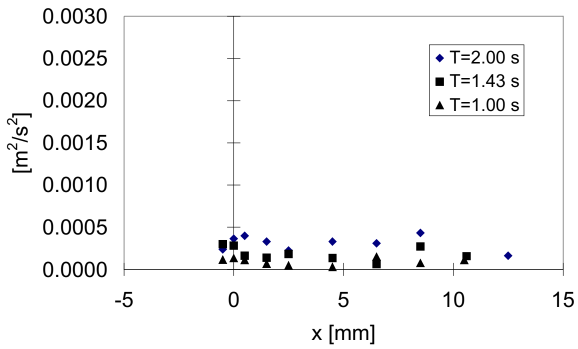

a) Cross section 10 mm from the nozzle.

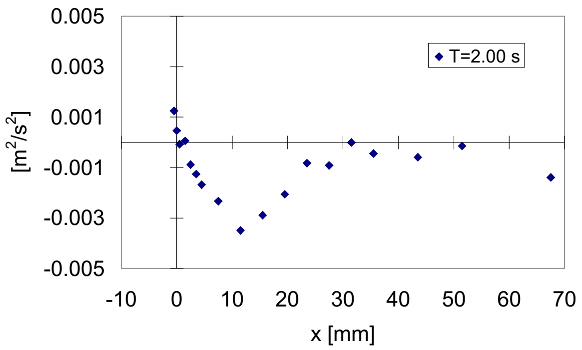

b) Cross section 60 mm from the nozzle.

Fig. 4. Continued

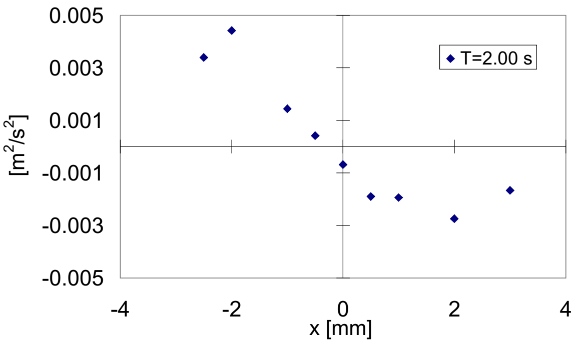

c) Cross section 110 mm from the nozzle.

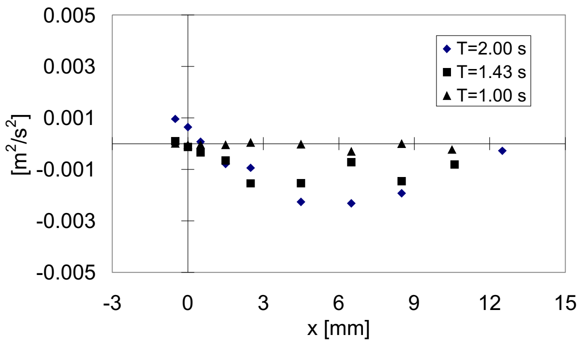

d) Cross section 160 mm from the nozzle.

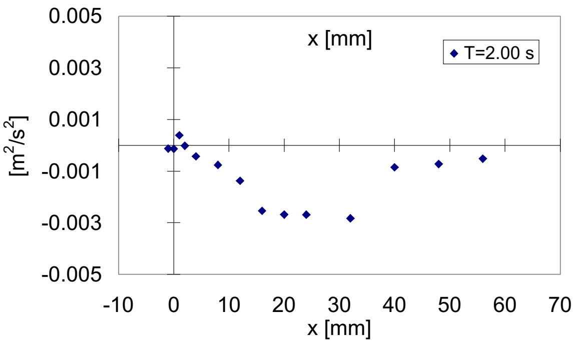

e) Cross section 210 mm from the nozzle.

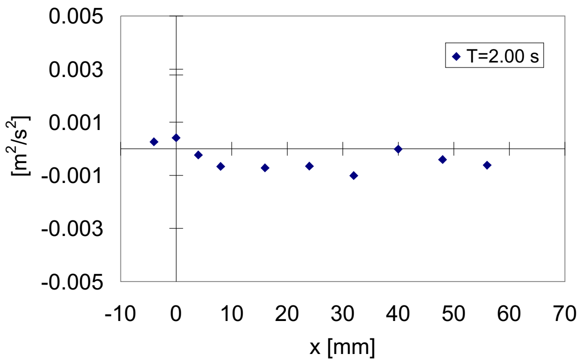

f) Cross section 260 mm from the nozzle.

Fig. 4. Cross-sectional profiles of $\overline{\widetilde{u}\widetilde{v}}$.

system in a time-averaged component, an oscillating component (statistical contribution of the wave) and a turbulent random component.

Results indicate the following:

1) Comparison of the root-mean square of turbulent velocity components indicates the effect of wave presence. Indeed, we observe that the root-mean square turbulent velocity component profiles of the sections close to the nozzle no longer presents a local minimum on the jet axis and that profiles tend to have lower values when the wave period diminishes. The root-mean square of turbulent velocity components for sections further from the nozzle are consistently greater than those of the same jet discharged in a stagnant ambient.
2) For cross sections further from the nozzle, the experimental values of shear turbulent Reynolds stresses indicate that, for configurations with the presence of wave motions, an inversion occurs of the sign compared to the jet issued in quiescent ambient. Shear wave Reynolds stresses diagrams are similar to that of shear turbulent Reynolds stresses of jets in still water, but their magnitude is smaller.
3) The root-mean square of the turbulent velocity components of jets in wave environment is greater than for the same jet in stagnant ambient, at least in cross sections particularly far from the nozzle.

REFERENCES

Chin D.A. (1987), "Influence of surface waves on outfall dilution", *ASCE Journal of Hydraulic Engineer,* 113 (8), pp. 1006-1017.

Chin D.A. (1988), "Model of buoyant-jet-surface-wave interaction", *ASCE Journal of Waterway, Port, Coastal and Ocean Engineering*, 114 (3), pp. 331-345.

Chyan J.M., Hwung', H.H. (1993), "On the interaction of a turbulent jet with waves", *Journal* of *Hydraulic Research*, 31 (6), pp. 791-810.

Ger A.M. (1979), "Wave effects on submerged buoyant jets", *Proceedings of the 8th Congress of the International Association for Hydraulic Research*, New Delhi, Part C, pp. 295-300.

Hussain A.K.M.F., Reynolds W.C. (1970), "The mechanics of an organized wave in turbulent shear flow", *Journal of Fluid Mechanics*, 41 (2), pp. 241-258.
Hwung H.H., Chyan J.M., Chang C.Y., Chen Y.F. (1994), "The dilution processes of alternative horizontal buoyant jets in wave motions", *Proceedings of the 24th Coastal Engineering Conference*, 5, pp. 3045-3059.
Le Méhauté B. (1969), "An introduction to hydrodynamics and water waves", *Water Wave Theories*, 2, TR ERL 118-POL-3-2, , Washington, D.C., U.S. Dept. of Commerce, ESSA
Koole R., Swan C. (1994a), "Measurements of a 2-D non-buoyant jet in a wave environment", *Coastal Engineering*, 24, pp. 151-169.
Koole R., Swan C. (1994b), "Dispersion of pollution in a wave environment", *Proceedings of the 24th Coastal Engineering Conference*, 5, pp. 3071-3085.
Mossa M. (1996), *Diffusione di un Getto in un Campo di Liquido in Quiete o in Moto Ondoso*, PhD thesis, Università degli Studi della Calabria, Cosenza, Italy (in Italian).
Mossa M., Petrillo A. (1997), "Turbulent energy transport of a jet in stagnant or wave environment", *Proceedings of the 27th Congress of the International Association for Hydraulic Research*, San Francisco, Theme B, vol. 1, pp. 173-178.
Rajaratnam N. (1976), *Turbulent Jets*, Amsterdam, Elsevier.
Shuto N. and Ti, L.H. (1974), "Wave effects on buoyant plumes", *Proceedings of the 14th Coastal Engineering Conference*, pp. 2199-2209.
Sharp J.J. (1986), "The effects of waves on buoyant jets", *Proc. Inst. Civ. Engineering*, 2 (81), pp. 471-475.
Wu S., Rajaratnam N., Katopodis C. (1998), "Oscillating vertical plane turbulent jet in shallow water", *IAHR Journal of Hydraulic Research,* 36 (2) , pp. 229-234.